

Article

Numerical Test and Strength Prediction of Concrete Failure Process Based on RVM Algorithm

Chunyang Xia ^{1,2,*} , Xuedong Guo ¹ and Wenting Dai ¹ ¹ Transportation College, Jilin University, Changchun 130000, China² School of Transportation, Changchun University of Architecture and Civil Engineering, Changchun 130000, China

* Correspondence: xiacy15@mails.jlu.edu.cn

Abstract: Recycled aggregate concrete (RAC) based on the machine learning (ML) method predicts the nonlinear uncertainty relationship between various mixing ratios and strength. Uniaxial compressive strength is one of the important indices to evaluate its performance. Machine learning is one of the essential methods for solving this nonlinear uncertainty relationship. To realize the selection of concrete raw materials and the learning and application of other influencing factors and provide guidance for engineering construction and application, this paper establishes a database of concrete uniaxial compressive strength based on Abaqus simulation software. The simulation results are highly consistent with the actual values. Based on the simulation database, with different water-cement ratios, different curing days, and recycled aggregate replacement rates as the input data set, the uniaxial compressive strength of concrete is the output data set. The data set is divided into a training set and a test set. A prediction model of the uniaxial compressive strength of concrete based on a relevance vector machine (RVM) algorithm is established. The results show that the maximum error between the simulated and experimental uniaxial compressive strength values is only 0.2 MPa. The correlation coefficient R between the predicted and simulated values of the concrete uniaxial compressive strength prediction model based on the RVM algorithm is 0.975. The model can effectively predict the compressive strength of RAC to meet the engineering requirements.

Keywords: Abaqus; relevance vector machine; concrete; strength; prediction



Citation: Xia, C.; Guo, X.; Dai, W. Numerical Test and Strength Prediction of Concrete Failure Process Based on RVM Algorithm. *Buildings* **2022**, *12*, 2105. <https://doi.org/10.3390/buildings12122105>

Academic Editors: Bingxiang Yuan, Yong Liu, Xudong Zhang, Yonghong Wang and Ahmed Senouci

Received: 30 September 2022

Accepted: 18 November 2022

Published: 1 December 2022

Publisher's Note: MDPI stays neutral with regard to jurisdictional claims in published maps and institutional affiliations.



Copyright: © 2022 by the authors. Licensee MDPI, Basel, Switzerland. This article is an open access article distributed under the terms and conditions of the Creative Commons Attribution (CC BY) license (<https://creativecommons.org/licenses/by/4.0/>).

1. Introduction

Concrete is an economical and widely used building material. As a new type of inorganic, non-metallic material, concrete has the characteristics of high plasticity, significant damping, stable mechanical properties, and easy access. Infrastructure, defence, construction, protection, and other fields have a comprehensive role [1–3].

Many scholars at home and abroad have done a lot of research on the performance of RAC and have produced a lot of research results [4–7]. By comparing the compressive strength and tensile strength of RAC and ordinary concrete, it is concluded that the compressive strength of RAC is slightly higher than that of standard concrete and the tensile strength is somewhat lower than that of ordinary concrete. Based on a large number of laboratory tests, it is concluded that when the replacement rate of recycled aggregate is 50%, the concrete strength reaches the maximum. Some scholars have studied the main factors affecting the compressive strength of concrete by compressive strength test combined with variance analysis on the concrete blocks produced after processing and processing of C30 blocks abandoned in the laboratory. Some scholars have studied the difference in mechanical properties of RAC and discussed the research direction of the mechanical properties of RAC in the future [8–14]. The surface of recycled aggregate is wrapped with a considerable amount of cement mortar, and the porosity of cement mortar is large, and the edges and corners are more porous; thus, its apparent density and bulk density cannot

reach the standard of natural aggregate, but it is conducive to earthquake resistance and reduces the weight of the structure.

With the development of engineering construction, the use environment of concrete is becoming more and more complex. The concrete preparation technology based on the traditional mix design method has been divorced from the development of modern concrete due to the limitation of manual experience and a large number of test batches [15–21]. To meet the needs of high-quality development of new building materials, effective prediction of concrete performance, and multi-directional performance optimization, it is urgent to explore and establish a scientific, intelligent, general, and efficient mix design technology system. The machine learning method is a new method to break through the limitations of the empirical regression model in a traditional mix design and predict the relationship between concrete mix proportion and performance because it has the characteristics of an extensive learning data set and artificial experience adjustment. This method has been paid attention to and applied in the seismic design of story buildings, intelligent urban planning, intelligent structural design, engineering health monitoring, production quality control, material strength prediction, and durability multi-objective mix proportion optimization in the field of civil engineering. The adopted algorithms mainly include artificial neural networks, support vector machines, and decision trees. Among them, the artificial neural network introduces nonlinearity by changing the excitation function and lifting the hidden layer number and usually selects cross-entropy as the loss function. The algorithm has strong adaptability but requires a lot of data training, making it difficult to explain the internal mechanism. Support vector machines introduce nonlinearity through kernel functions. Usually, it selects the page closure loss function intending to maximize the boundary, which has excellent nonlinear separability, but the kernel function is sensitive and challenging to train. A decision tree has strong generalization ability but is accessible to over-fitting by constructing the tree's structure and circulating the feature segmentation process. Each algorithm needs to be combined with different data situations to solve specific problems. Some scholars have studied the application of artificial neural networks to the strength prediction of RAC. Compressive strength, as one of the leading performance indices of RAC, is related to the incorporation rate of recycled aggregate, water-cement ratio, and age. Moreover, the compressive strength of concrete belongs to destructive and non-repeatable tests, and each strength test requires at least three samples of the same sample, which is laborious and time-consuming. If a virtual simulation test of concrete's compressive strength can be established and a stable and reliable prediction model can be established, the destructive test can be avoided. It is difficult and complex to establish a multi-factor compressive strength equation for RAC by the analytical method. Compressive strength is the most basic and essential mechanical property of concrete and is also the key factor to consider in the design of a concrete structure. There are also corresponding empirical prediction models in the entire public data and standard specifications, which can provide the basis for the prediction based on raw materials and mixture ratio [22–24]. In recent years, it has aroused great interest to construct the potential relationship between the uniaxial compressive strength of concrete and its influencing factors in a new way. That is to say, a new model can be constructed to learn the potential characteristics of the data through the existing database and predict the uniaxial compressive strength.

At present, domestic and foreign scholars have carried out some explorations in predicting the compressive strength of concrete by machine learning methods. Because of the large data sets and laboratory data sets used in practical engineering, three main types of machine learning methods are used to predict the 28-day compressive strength of ordinary concrete and evaluate the actual performance of the data set model. Sensitivity analysis, grey correlation analysis, BP neural network weight importance analysis, and Mahalanobis distance method are used to determine the influence of different strength-influencing factors on the compressive strength of concrete from a single perspective. The prediction accuracy of the 28-day compressive strength of experimental concrete, recycled aggregate concrete, and highway concrete at the University of California, Irvine is comprehensively

analyzed by using a support vector machine model and a random forest model based on a decision tree compared with an artificial neural network model. In addition, some scholars have also done further work on the algorithm model. For example, the adaptive neuro-fuzzy inference system (ANFIS) combined with an artificial neural network model and fuzzy inference model (FL) can provide expert knowledge by using FL based on an artificial neural network. The performance of ANFIS has been effectively tested in predicting the compressive strength of experimental concrete and concrete containing blast furnace slag and fly ash at the University of California, Irvine. The optimization neural network model combined with the meta-heuristic algorithm is also widely used. Based on an artificial neural network, a multi-objective grey wolf optimization algorithm and an improved firefly algorithm are combined to predict the compressive strength of concrete containing silica fume and high-performance concrete. For the prediction of compressive strength of high-performance concrete, the FA-LSSVR hybrid model and the ECSO-SVM hybrid model based on a support vector machine are adopted, which have higher prediction accuracy and stronger robustness. The XGBoost model developed on the traditional tree gradient lifting method predicts the compressive strength of concrete laboratory data sets, and XGBoost shows the strong ability of structured data sets. The machine-learning method offers substantial advantages in the prediction of concrete strength [25–31]. SVM often needs to use a cross-validation method to determine the model complexity parameter C . For RVM, another advantage of introducing the Bayesian method is that it eliminates the step of model selection. RVM introduces Bayesian methods to provide the output of posterior probabilities and often produces sparser solutions (faster prediction on test sets). ABAP ATHY et al. [32] used statistical models to predict the strength of fiber-reinforced concrete based on concrete strength tests with different fiber volume fractions. MILAN et al. [33] predicted the compressive strength of self-compacting concrete based on a single and an ensemble model. They found that the artificial neural network model in the ensemble model has higher accuracy.

To sum up, the current research has achieved some results. However, there are still data sets, generally less single, not effectively combined with the characteristics of the data set itself to explore the impact of characteristic parameters on compressive strength from multiple perspectives. There are many models for predicting concrete strength by machine learning algorithms in the study, which makes the quality of the original data samples have an essential impact on the model's prediction ability. To avoid this defect, the simulation module is added in this paper, which reduces the problem of a long cycle of obtaining original samples caused by the test so that a large number of sample data sets can be created to meet different working conditions. Based on this, this paper selects the relevant vector machine model. Firstly, the uniaxial compressive strength database of concrete is established by Abaqus simulation software, and the uniaxial compression test verifies the simulation data. The simulation results are in good agreement with the actual values. Then based on the simulation database, the water-cement ratio, different curing days, recycled aggregate replacement rate as the input data set, different curing days of concrete uniaxial compressive strength as the output data set, and 38 sets of data sets are divided into a training set and test set. The Bayesian method is introduced to provide the posterior probability output and generate a sparser solution (faster prediction on the test set). A prediction model of concrete uniaxial compressive strength based on the RVM algorithm is established to provide a reference for predicting concrete uniaxial compressive strength.

2. Materials and Methods

2.1. Material

The laboratory waste C30 concrete test block, using the model of a PE60 × 100 jaw crusher for crushing, washing, and screening, take 5~31.5 mm continuous particle size recycled coarse aggregate. The cementitious material used in this experiment is P.O. 42.5 ordinary Portland cement; for its chemical properties and physical properties, see Table 1.

Table 1. Physical and Chemical Properties of Portland Cement.

Category	Burning Vector/%	w(MgO)/%	w(SO ₃)/%	Initial Setting Time/min	Final Coagulation Time/min
Content	3.4	2.65	3.0	95	550

2.2. Mechanical Properties Test

Firstly, based on the design method of ordinary concrete mix proportion, the mix proportion of C30 RAC is calculated, and the effective water absorption of recycled aggregate is combined with increasing the additional water. Secondly, according to the concrete test operation rules, the mixed concrete is poured into the 150 mm × 150 mm × 150 mm test mould for mechanical vibration. After the vibration is uniform and dense, it is put into the standard maintenance room. The temperature is (20 ± 2) °C, and the relative humidity is greater than 95%. A total of 9 test blocks are shown in Figure 1.

**Figure 1.** Concrete block.

The WEW-1000A universal testing machine was used for the loading test. The loading speed is 0.5~1.0 MPa/s. See Table 2 for the strength of concrete blocks. Water-to-cement ratio a , different curing days d , recycled aggregate replacement rate r , and concrete uniaxial compressive strength f_{ck} . The higher the compressive strength of concrete is, the less compressive deformation that can be endured during compression failure. When the ultimate load is reached, the concrete is suddenly destroyed, the brittleness is obvious, and the degree of development of internal cracks is also better. Before reaching the peak strength, there was no obvious crack on the surface of the test block; however, after reaching the peak strength, the accumulated energy inside the test block rapidly releases to produce damage and a burst sound. However, due to the ductility of concrete, the test block can withstand relatively large compression deformation after failure, and its integrity is preserved.

Table 2. Results of uniaxial compressive strength of concrete blocks.

No.	a	d	r	f_{ck}/MPa
1	0.43	3	0.43	23.8
2	0.43	7	0.43	30.2
3	0.43	28	0.43	35.7
4	0.49	3	0.43	21.7
5	0.49	7	0.43	24.2
6	0.49	28	0.43	32.9
7	0.55	3	0.43	21.0
8	0.55	7	0.43	24.2
9	0.55	28	0.43	29.1

2.3. Construction of Simulation Database Based on Abaqus

With the continuous development of computers and finite elements, researchers combine the improved cohesion model with finite elements to study the fracture problems of various materials, such as composite materials, rocks, and concrete. The constitutive models of concrete in ABAQUS include the brittle crack model, stain crack model, and plastic damage model. The concrete plastic damage model is based on the continuum damage model in plasticity theory. It is assumed that the concrete damage is caused by tensile cracking and compression failure. In the deformation process, the factors of crack propagation and closure are added. The usual flow rules of stiffness degradation and recovery in reciprocating loading and unloading are non-associated flow rules. At the same time, the plastic damage model of concrete takes into consideration the tensile–compressive softening effect of concrete. This model is also the only one that can be used for both ABAQUS/Standard and ABAQUS/explicit analysis modules.

To obtain more uniaxial compressive strength values of RAC specimens under different ratios, Abaqus is used to simulate the uniaxial compressive strength values of RAC models under different ratios. The cube test block of 150 mm × 150 mm × 150 mm used in this paper does not consider friction at the end of the simulation analysis. In terms of load setting, the y-direction force is applied, and the bottom is fixed. Good meshing must depend on good geometric structure, and pre-processing is the most critical and essential work in finite element analysis. The modelling based on engineering problems is transformed into an analysis model, completed in the pre-processing, involving geometric processing, material sets, mesh generation, boundary application, and other related steps. Only when these steps are well done can a correct result output be ensured. The Hypermesh pre-processing software is used to mesh and optimize the numerical model of concrete. Its powerful geometric processing function can quickly read the model data with its complex structure and large scale and adapt to the complex boundary. After setting the whole mesh, the details can be processed and optimized to obtain a more reasonable mesh distribution, which greatly improves the efficiency of finite element calculation. The model grid is divided and optimized by Hypermesh, such as in Figure 2. The concrete constitutive model of the GB50010-2010 Code for the design of concrete structures is selected [27].

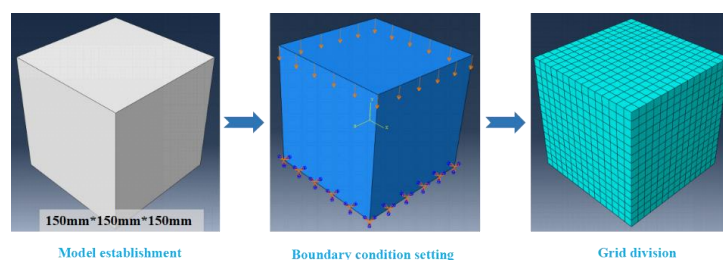


Figure 2. Establishment of concrete block model based on Abaqus.

The loading mode is similar to uniaxial compression in the laboratory. The specimen is loaded by displacement, that is, by controlling the node displacement of the solid element on the top surface. The specimen has only one boundary constraint mode, which is that the vertical displacement of the bottom surface of the specimen is 0.

The model (Figure 2) includes a concrete test block with the size of 150 mm × 150 mm × 150 mm. The correctness of the concrete constitutive model is verified by simulating the mechanical properties of the concrete test block under uniaxial compression. The concrete test blocks were divided into 19,173 elements by sweeping with the four-node linear tetrahedral element (C3D4). The viscous element is divided into 19,173 units by a four-node three-dimensional bonding element (COH3D6).

Figure 3 shows the compression of RAC blocks at different time steps under No. 2 working conditions. It can be seen that the process is similar to the compression process of the test block. To verify the accuracy of the simulation results, the compression simulation of No. 1~9 test blocks was carried out under the same test conditions. The results show

that the maximum error between the simulation results and the uniaxial compression test results of 9 groups of concrete blocks is 0.2 MPa, as shown in Figure 4.

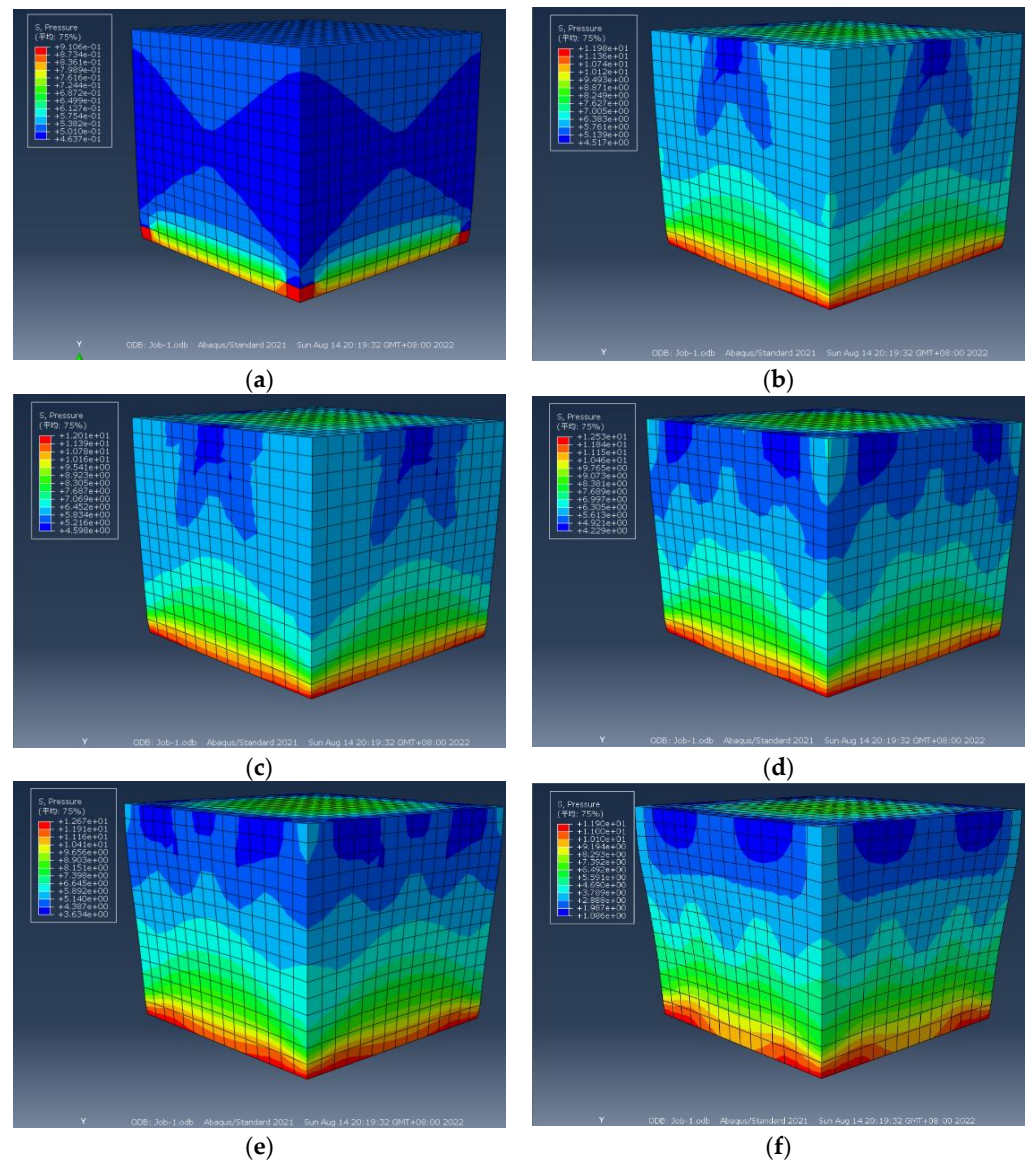


Figure 3. Compression of concrete test blocks at different time steps. (a) step 1. (b) step 10. (c) step 20. (d) step 30. (e) step 40. (f) step 50.

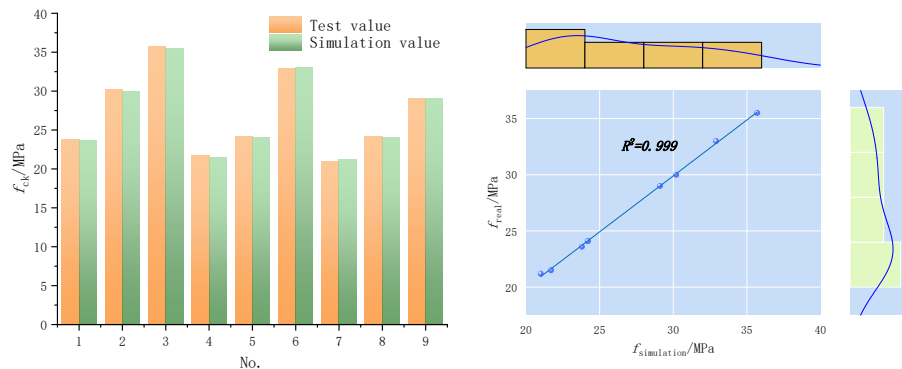


Figure 4. Comparison of test and simulation values.

The failure of concrete blocks is divided into four processes: the compaction process, the elastic deformation process, the elastic-plastic deformation process, and the failure process.

Step. 1 After loading, the load of the sample increases a little with the increase in displacement. In the numerical simulation analysis, the deformation of the specimen in the laboratory at this stage is obviously larger than that of the specimen. The existence of this stage in the laboratory test block is mainly due to the existence of a micro-concave-convex zone on the surface of the concrete test block prepared in the laboratory and the gradual compaction of micro-cracks and micro-pores in the concrete test block. However, the simulated specimen is caused by the top-down transfer of axial pressure and the compaction of the concrete element and the non-thickness bond element. The specimen element does not deform under compression.

Step. 2 With the increase in axial load, it can be seen from the cloud picture that the thicknesses of the bond unit on the left and right surfaces of the specimen have been deformed, and the concrete unit has not been significantly deformed macroscopically, but small cracks have begun to appear locally, which is in good agreement with the test.

Step. 3 The solid element in the lower right corner of the specimen has begun to slowly peel away from the specimen, and the thickness of the adhesive element mesh has been severely compressed and gradually lost its adhesive ability.

Step. 4 With the increased plastic deformation of the specimen, the axial load no longer increases, and the specimen is damaged, which is consistent with the test results. From the displacement nephogram, it can be seen that the concrete element on the surface of the specimen gradually falls off from the surface or interior of the model, and the deformation of the thickness bonding element is intensified until it disappears.

Figure 4 shows that the error between the numerical simulation results and the experimental results is within 0.2 MPa. The calculation of the uniaxial compressive strength of the mixed soil by the model in this paper is in good agreement with the measured value. The correlation coefficient R^2 between the two data is as high as 0.999.

Water cement ratio a , different curing days d , recycled aggregate replacement rate r as input data set, concrete uniaxial compressive strength f_{ck} as output data set. Before the modeling of data samples, all the imported data were normalized to realize the principle of dimensional analysis. The simulation database is shown in Table 3:

$$x' = 2 \times \frac{x - x_{\min}}{x_{\max} - x_{\min}} - 1 \quad (1)$$

where x is the original data, x' is the normalized data, x_{\max} is the maximum value of the original data, and x_{\min} is the minimum value.

Table 3. Simulation database.

No.	a	d	r	f_{ck}
1	0.2	3	0.38	0.35
2	0.2	7	0.38	0.50
3	0.2	28	0.38	0.65
4	0.5	3	0.38	0.26
5	0.5	7	0.38	0.43
6	0.5	28	0.38	0.58
7	0.8	3	0.38	0.24
8	0.8	7	0.38	0.31
9	0.8	28	0.38	0.54
10	0.2	3	0.50	0.39
11	0.2	7	0.50	0.53
12	0.2	28	0.50	0.69
13	0.5	3	0.50	0.42
14	0.5	7	0.50	0.55
15	0.5	28	0.50	0.71

Table 3. Cont.

No.	a	d	r	f_{ck}
16	0.8	3	0.50	0.29
17	0.8	7	0.50	0.37
18	0.8	28	0.50	0.63
19	0.2	3	0.62	0.27
20	0.2	7	0.62	0.39
21	0.2	28	0.62	0.51
22	0.5	3	0.62	0.23
23	0.5	7	0.62	0.32
24	0.5	28	0.62	0.50
25	0.8	3	0.62	0.20
26	0.8	7	0.62	0.25
27	0.8	28	0.62	0.46
28	0.2	3	0.20	0.45
29	0.2	7	0.35	0.40
30	0.3	28	0.80	0.21
31	0.2	3	0.20	0.80
32	0.2	7	0.35	0.79
33	0.3	28	0.80	0.62
34	0.2	3	0.20	0.45
35	0.2	7	0.38	0.40
36	0.2	28	0.50	0.35
37	0.2	3	0.62	0.37
38	0.2	7	0.80	0.35
39	0.2	7	0.35	0.45
40	0.2	28	0.80	0.40
41	0.3	3	0.20	0.35
42	0.2	7	0.38	0.37
43	0.2	28	0.50	0.35
44	0.2	3	0.62	0.36
45	0.2	7	0.80	0.39

3. Construction of Concrete Mechanics Model Based on RVM

3.1. Theory of RVM Method

The relevance vector machine (RVM) is a sparse probability model proposed by Tipping on the basis of a support vector machine (SVM). It is trained in the Bayesian framework by defining the Gaussian prior probability controlled by the super parameter α on the weight ω . In the iterative process of sampling data, the posterior distribution of most parameters tends to zero, and the automatic relevance determination (ARD) is used to remove these points independent of the predicted value so as to obtain the sparse model. RVM has high sparsity, which can not only obtain binary output but also give a prediction probability. RVM can not only achieve the same prediction accuracy as SVM but also greatly reduce the calculation amount of the kernel function and shorten the prediction time, which is more suitable for online prediction. In addition, RVM does not need to satisfy Mercer's theorem in kernel function selection, so it has better generalization ability and has broad application prospects in predictive control, pattern recognition, and multi-domain prediction. This chapter briefly introduces the basic principles and model derivation process of the RVM algorithm. The Bayesian learning theory is developed on the basis of Bayes' theorem. It is a process of using probability to represent all forms of uncertainty and realizing learning and reasoning through probability rules. Bayesian learning uses the prior distribution of parameters and the posterior distribution obtained from sample information to obtain the overall distribution. As the basis of the Bayesian learning framework, Bayes' theorem plays an important role in linking event prior and posterior probability [34,35].

It is applied to regression prediction analysis, and a sparse model is obtained in data training, ignoring some irrelevant data points, thereby reducing the amount of calculation.

Assuming that the original data set used for training is $\{x_n, t_n \mid n = 1, 2, \dots, N\}$, x_n representing the sample input vector used for training, and t_n representing the output vector of independent distribution, the functional relationship between x_n and t_n is established.

$$t_n = y(x_n; \omega) + \xi_n \quad (2)$$

In the formula, ξ_n is the additional Gaussian noise satisfying $\xi_n \sim N(0, \sigma^2)$, and σ^2 is the amount to be solved. It can be inferred that the following equation needs to satisfy the Gaussian distribution.

$$p(t_n \mid x) = N(t_n \mid y(x_n), \sigma^2) \quad (3)$$

In the formula, the size of t_n depends on $y(x_n)$ and σ^2 , since t_n is non-interference and independent, the likelihood function of training and data can be expressed as follows

$$P(t \mid \omega, \sigma^2) = (2\pi\sigma^2)^{-N/2} \exp\left\{-\frac{1}{2\sigma^2} \|t - \Phi\omega\|^2\right\} \quad (4)$$

In the formula, $t = (t_1, t_2, \dots, t_N)^T$, $\omega = (\omega_0, \omega_1, \dots, \omega_n)^T$, Φ , and $N \times (N + 1)$ are matrices, ω satisfy the Gaussian distribution with a priori distribution mean of 0 and variance of α_i^{-1} , and then deduce the following formula.

$$P(\omega \mid \alpha) = \prod_{n=0}^N N(\omega_n \mid 0, \alpha_n^{-1}) \quad (5)$$

In the formula, hyperparameter $\alpha = (\alpha_0, \alpha_1, \dots, \alpha_N)^T$, each α_i has a corresponding ω_i , and the training set sample data set can be prior distributed. According to Bayesian principle, the expression of posterior distribution can be obtained by weight ω_i as follows:

$$P(t \mid \omega, \alpha, \sigma^2) = \left\{ \begin{array}{l} = \frac{P(t \mid \omega, \sigma^2) P(\omega, \alpha)}{P(t \mid \alpha, \sigma^2)} \\ = (2\pi)^{-(N+1)/2} |\Sigma|^{-1/2} \exp\left\{-\frac{1}{2}(\omega - \mathbf{m})^T \Sigma^{-1}(\omega - \mathbf{m})\right\} \end{array} \right\} \quad (6)$$

where $\mathbf{m} = \sigma^2 \Sigma \Phi^T t$, $\Sigma = (\sigma^{-2} \Phi^T \Phi + \mathbf{A})^{-1}$.

$\mathbf{A} = \text{diag}(\alpha_0, \alpha_1, \dots, \alpha_N)$ Finally, the maximum likelihood function can be expressed by the following formula.

$$P(t \mid \alpha, \sigma^2) = \left\{ \begin{array}{l} = \int P(t \mid \omega, \sigma^2) P(\omega \mid \alpha) d\omega \\ = (2\pi)^{-N/2} |C|^{-1/2} \exp\left(\frac{1}{2} t^T C^{-1} t\right) \end{array} \right\} \quad (7)$$

C is covariance, pair and derivation, with a value of 0, you can get the following two expressions:

$$\alpha'_i = \frac{r_i}{\mu_i^2} \quad (8)$$

$$(\sigma') = \frac{\|t - \Phi\mu\|^2}{N - \sum_i r_i} \quad (9)$$

where μ_i is the i th posteriori average weight and r_i is the element on the i th principal diagonal.

The design idea of a regression prediction model of concrete strength based on RVM is shown in Figure 5. The water-cement ratio, maintenance days, and replacement rate were used as input layer indices, and the compressive strength at 3 d, 7 d, and 28 d was used as output layer indices. Five groups of samples were selected to test the prediction error of the model. Finally, the number of neurons is determined, and the trained network is preserved. The RVM concrete strength prediction model is used to predict the expansion degree and compressive strength of fill materials with different proportions.

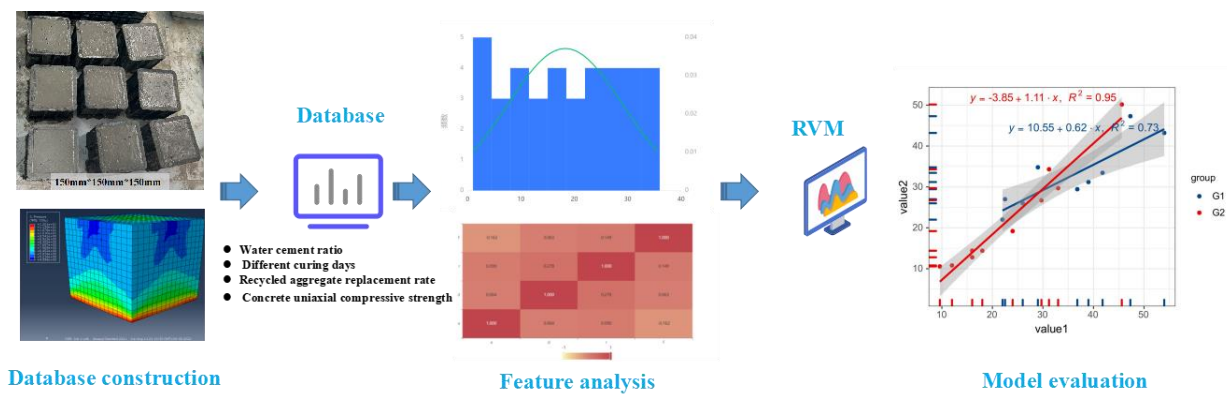


Figure 5. Regression prediction process of concrete strength based on RVM.

3.2. Data Set Analysis

In order to investigate the correlation between indicators, the statistical information and correlation of sample indicators were analyzed. In Figure 6, the probability density curve of the sample index distribution shows whether the data conforms to a normal distribution. The results show that the data for each sample index is non-normal distribution. In addition, Figure 7 shows that the correlation between most input indicators is weak ($R < 0.5$). Therefore, the input indicators are independent of each other. The correlation analysis of the sample input data is shown in Figure 7. The overall new description of Shapiro-Wilk small data for the data is shown in Table 4. Each input index in Table 4 shows significance, rejecting the null hypothesis, and the kurtosis of a sample, d sample, and R sample is -1.273 , -1.408 , -0.167 (absolute value is less than 10), and the absolute value of skewness is less than 3. Therefore, the indicators in the data do not satisfy the normal distribution. However, the output indicator's $f p$ value for significance is 0.101; the level does not present the significance and cannot reject the null hypothesis. Therefore, this indicator satisfies the normal distribution.

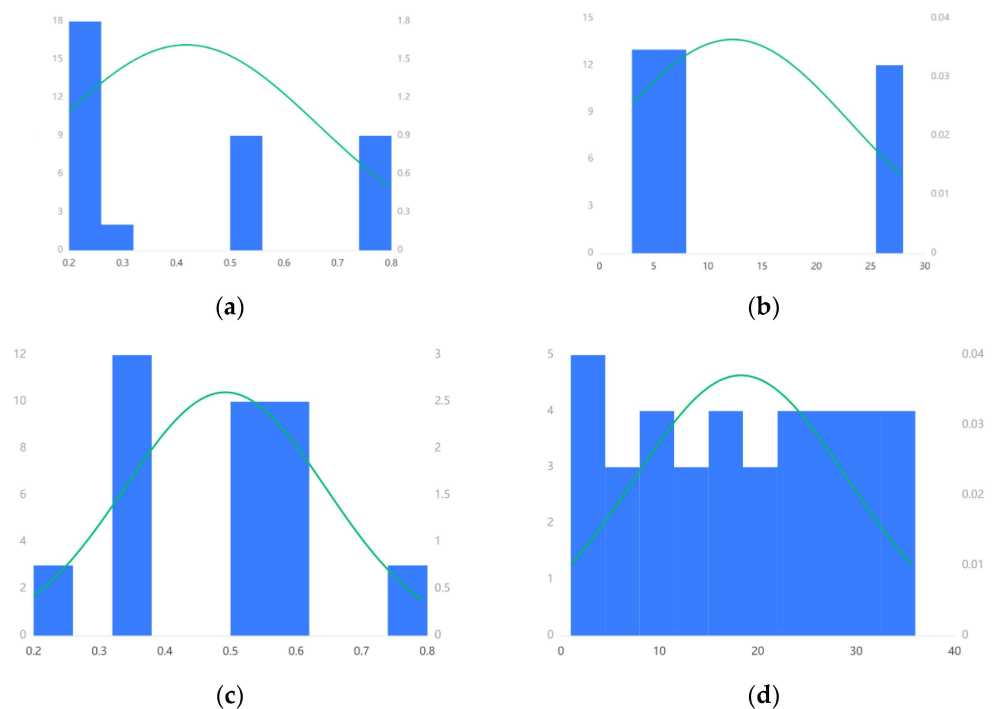


Figure 6. Database normality test histogram. (a) a-Normality test histogram. (b) d-Normality test histogram. (c) r-Normality test histogram. (d) f-Normality test histogram.

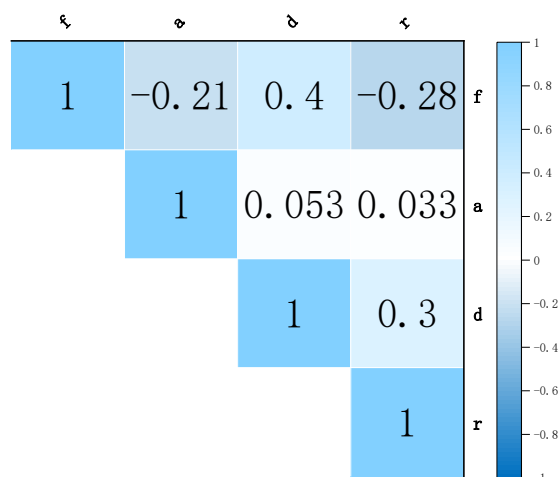


Figure 7. Thermal graph of sample feature correlation matrix.

Table 4. Relevant mechanical indexes of concrete. Asterisk shows the Relevant mechanical indexes of concrete. More asterisk show more relevance.

Variable Name	Skewness	Kurtosis	S-W Test
a	0.595	0.758 (0.000) ***	0.35
d	0.748	0.683 (0.000) ***	0.50
r	0.11	0.926 (0.015) **	0.65
f	-0.041	0.952 (0.101)	0.39

Figure 7 is the correlation for each sample. Water-to-cement ratio and recycled aggregate are the key factors affecting the strength of concrete, while the influence of curing time on the strength of RAC is not obvious. Figure 7 shows that the absolute value of the correlation between the items is less than 0.4, showing a low correlation between the indicators. From the correlation between the input index and the output index, the d-sample index has a higher impact on the output index than the r-sample.

3.3. Results and Analysis

Finally, the predicted value is shown in Table 5. From the test results of the support vector regression model in Table 5, it can be seen that three of the errors between the calculated value and the simulation value are higher than 0.09, and most of the errors of the samples are within 0.09. It can be seen that the accuracy of the correlation vector regression model is beyond doubt. It can be considered that the correlation vector regression model has good generalization ability when dealing with small sample data, so it can be effectively used for processing experimental data analysis.

Table 5. Predictive value and simulation value.

No.	Simulation- f_{ck}	RVM Prediction- f_{ck}	Errorl
34	0.45	0.444	0.006
35	0.40	0.408	0.008
36	0.35	0.340	0.010
37	0.37	0.360	0.010
38	0.35	0.360	0.010
39	0.45	0.444	0.006
40	0.40	0.408	0.008
41	0.35	0.340	0.010
42	0.37	0.360	0.010
43	0.35	0.360	0.010
44	0.36	0.361	0.001
45	0.39	0.387	0.003

To better show the relationship between the compressive strength of concrete calculated by the support vector regression model and the simulation value, as shown in Figure 8, it can be seen from the figure that the sample points are all located near the straight line with a slope of 1.

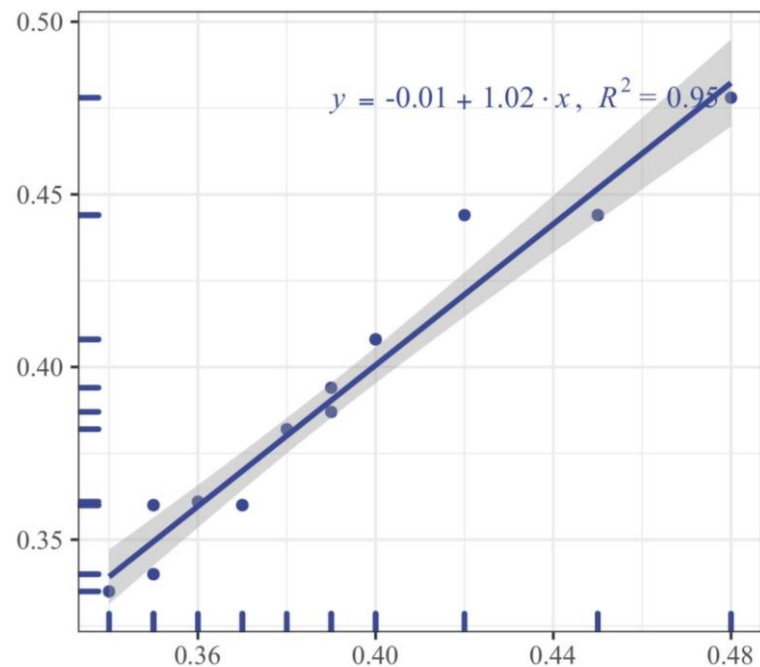


Figure 8. Fitting curve of simulation value and predicted value.

The study adds common model evaluation metrics to more intuitively evaluate the model's performance in Table 6. These criteria included the coefficient of determination (R^2), root mean square error (RMSE), standard deviation (SD), and mean absolute percentage error (MAPE), as shown in Table 6. The greater the R^2 , the closer the slope of the model fitting line is to 1, and the more accurate the prediction of concrete's compressive strength is.

$$R^2 = 1 - \frac{\sum_{i=1}^n (f_{\text{real}} - f_{\text{pred}})^2}{\sum_{i=1}^n (f_{\text{real}} - \bar{f}_{\text{pred}})^2} \quad (10)$$

$$\text{RMSE} = \sqrt{\frac{\sum_{i=1}^n |f_{\text{real}} - f_{\text{pred}}|^2}{n}} \quad (11)$$

$$\text{SD} = \sqrt{\frac{\sum_{i=1}^n (f_{\text{pred}} - \bar{f}_{\text{pred}})^2}{n}} \quad (12)$$

$$\text{MAPE} = \frac{1}{n} \sum_{i=1}^n \left| \frac{f_{\text{real}} - f_{\text{pred}}}{f_{\text{real}}} \right| \times 100\% \quad (13)$$

Table 6. Model evaluation.

Model	No.	Test			
		R^2	RMSE	SD	MAPE
RVM	34~45	0.9506	0.0074	0.5779	1.53%

By establishing a concrete strength prediction model based on the RVM model, although the prediction accuracy of RAC uniaxial compressive strength is high, there is still a problem of insufficient initial sample data. There is no comparative analysis of various machine learning models. Through the comparative analysis of various models, the optimal model can be obtained to predict the uniaxial compressive strength of RAC.

4. Conclusions

In this paper, the application of machine learning to concrete is studied, and the model of RAC compressive strength with coarse aggregate replacement rate, water–cement ratio, and curing time based on the RVM model is established. The article draws the following conclusions.

(1) The application of RAC materials is the key point. Firstly, the uniaxial compressive strength test of nine RAC blocks with different substitution rates, water-cement ratios, curing times, and other factors is carried out, and the properties of their basic materials are determined, which establishes the foundation for ABAQUS-based simulation analysis.

(2) A database of RAC strength is established based on Abaqus software, which provides a data basis for the subsequent concrete strength prediction model based on the machine learning method. The maximum error between the simulation results and the uniaxial compressive test results of nine groups of concrete blocks is 0.2 MPa, which verifies the correctness of the simulation database. Finally, 45 groups of concrete uniaxial compressive strength values were obtained under different replacement rates, water cement ratios, and curing times.

(3) With 45 training samples as an input data set and uniaxial compressive strength as an output data set, the RVM prediction model was established. After training and learning, the training efficiency is greatly improved, and the error is small when testing the test samples. Combined with the regression fitting coefficient $R^2 = 0.9506$, it is further demonstrated that the model can effectively predict the compressive strength of RAC and meet the engineering requirements. The model can be generalized and applied.

Author Contributions: Conceptualization, C.X. and W.D.; methodology, C.X. and X.G.; validation, C.X. and W.D.; writing—original draft preparation, C.X. All authors have read and agreed to the published version of the manuscript.

Funding: This research received no external funding.

Data Availability Statement: The data are all included in this manuscript.

Conflicts of Interest: The authors declare no conflict of interest.

References

1. You, F.; Luo, S.; Zheng, J. Experimental study on residual compressive strength of recycled aggregate concrete under fatigue loading. *Front. Mater.* **2022**, *9*, 13. [[CrossRef](#)]
2. Kim, D.K.; Chang, S.K.; Sang, K.C. Advanced Probabilistic Neural Network for the Prediction of Concrete Strength. *Icces* **2007**, *2*, 29–34. [[CrossRef](#)]
3. Liu, C.Y.; Wang, Y.; Hu, X.M.; Han, Y.L.; Zhang, X.P.; Du, L.Z. Application of GA-BP neural network optimized by Grey Verhulst model around settlement prediction of foundation pit. *Geofluids* **2021**, *2021*, 5595277. [[CrossRef](#)]
4. Lee, J.J.; Kim, D.K.; Chang, S.K.; Lee, J.H. Application of support vector regression for the prediction of concrete strength. *Comput. Concr.* **2007**, *4*, 299–316. [[CrossRef](#)]
5. Al-Attar, T. Development of Mathematical Models for Prediction of Structural Concrete Strength. Ph.D. Thesis, College of Engineering, University of Baghdad, Baghdad, Iraq, 2001.

6. Nguyen, H.; Vu, T.; Vo, T.P.; Thai, H.T. Efficient machine learning models for prediction of concrete strengths. *Constr. Build. Mater.* **2021**, *266*, 120950. [[CrossRef](#)]
7. Liu, C.; Du, L.; Zhang, X.; Wang, Y.; Hu, X.; Han, Y. A New Rock Brittleness Evaluation Method Based on the Complete Stress-Strain Curve. *Lithosphere* **2021**, *2021*, 4029886. [[CrossRef](#)]
8. Ly, H.B.; Nguyen, M.H.; Pham, B.T. Metaheuristic optimization of Levenberg–Marquardt-based artificial neural network using particle swarm optimization for prediction of foamed concrete compressive strength. *Neural Comput. Appl.* **2021**, *33*, 17331–17351. [[CrossRef](#)]
9. Wu, X.; He, Q.; Zheng, P.; Xiao, K.L. Influence Analysis of Concrete Strength on Time-Varying Reliability of Widening T-Beam Bridge Based on Support Vector Method. *J. Chongqing Jiaotong Univ. (Nat. Sci.)* **2019**, *38*, 33–38.
10. Wu, D.-Y. Influence of maintain duration on prediction of concrete strength by rebound method. *J. Anhui Inst. Archit.* **2005**, *5*, 8–10.
11. Zain, M.F.M.; Abd, S.M.; Sopian, K.; Jamil, M.; Che-Ani, A.I. Mathematical regression model for the prediction of concrete strength. In Proceedings of the 10th WSEAS International Conference on Mathematical Methods, Computational Techniques and Intelligent Systems, Sofia, Bulgaria, 2–4 May 2008.
12. Sharifi, J.; Nikodel, M.R. Prediction of Concrete Strength Containing Different Aggregates through Artificial Neural Networks. *J. Eng. Geol.* **2015**, *9*, 2983–3002. [[CrossRef](#)]
13. Karaman, K.; Bakhytzhana, A. Prediction of concrete strength from rock properties at the preliminary design stage. *Geomech. Eng.* **2020**, *23*, 115–125. [[CrossRef](#)]
14. Shariati, M.; Mafipour, M.S.; Mehrabi, P.; Ahmadi, M.; Wakil, K.; Trung, N.T.; Togholi, A. Prediction of concrete strength in presence of furnace slag and fly ash using Hybrid ANN-GA (Artificial Neural Network-Genetic Algorithm). *Smart Struct. Syst.* **2020**, *25*, 183–195. [[CrossRef](#)]
15. Lin, W.; Bo, Y.; Abraham, A. Prediction of Concrete Strength Using Floating Centroids Method. In Proceedings of the IEEE International Conference on Systems, Manchester, UK, 13–16 October 2013. [[CrossRef](#)]
16. Rajasekaran, S.; Lee, S.C. Prediction of concrete strength using serial functional network model. *Struct. Eng. Mech.* **2003**, *16*, 83–99. [[CrossRef](#)]
17. Carino, N.J. Prediction of potential concrete strength at later ages. *ASTM Spec. Tech. Publ.* **1994**, *169*, 140–152.
18. Han, C.G.; Joo, E.H. Rapid Evaluation Method for Blast Furnace Slag Fineness and Influence of Fineness on Properties of Cement Mortar. *J. Archit. Inst. Korea Struct. Constr.* **2018**, *34*, 13–18. [[CrossRef](#)]
19. Kaloop, M.R.; Roy, B.; Chaurasia, K.; Kim, S.M.; Jang, H.M.; Hu, J.W.; Abdelwahed, B.S. Shear Strength Estimation of Reinforced Concrete Deep Beams Using a Novel Hybrid Metaheuristic Optimized SVR Models. *Sustainability* **2022**, *14*, 5238. [[CrossRef](#)]
20. Hong, J.; Miao, C. Study on prediction of concrete strength using wavelet neural network. *Ind. Constr.* **2004**, *34*, 47–49.
21. Uddin, M.N.; Li, L.Z.; Khan, R.K.M.; Shahriar, F.; Sob, L.W.T. Axial Capacity Prediction of Concrete-Filled Steel Tubular Short Members Using Multiple Linear Regression and Artificial Neural Network. *Mater. Sci. Forum* **2021**, *1047*, 220–226. [[CrossRef](#)]
22. Wang, X.; Dong, S.; Ashour, A.; Han, B. Bond of nano inclusions reinforced concrete with old concrete: Strength, reinforcing mechanisms and prediction model. *Constr. Build. Mater.* **2021**, *283*, 122741. [[CrossRef](#)]
23. Wang, X.; Liu, Y.; Xin, H. Bond strength prediction of concrete-encased steel structures using hybrid machine learning method. *Structures* **2021**, *32*, 2279–2292. [[CrossRef](#)]
24. Assis, L.S.D.; Assis, J.T.D.; Pessoa, J.R.D.C.; Tavares Júnior, A.D. Elaboration of fracture prediction map using 2D digital image correlation—2D CID. *Rev. IBRACON Estrut. Mater.* **2022**, *15*, 1–9. [[CrossRef](#)]
25. Razzaghi, H.; Madandoust, R.; Aghabarati, H. Point-load test and UPV for compressive strength prediction of recycled coarse aggregate concrete via generalized GMDH-class neural network. *Constr. Build. Mater.* **2021**, *276*, 122143. [[CrossRef](#)]
26. Zhu, L.; Zhao, C.; Dai, J. Prediction of compressive strength of recycled aggregate concrete based on gray correlation analysis. *Constr. Build. Mater.* **2021**, *273*, 121750. [[CrossRef](#)]
27. Zulkarnain, M.; Mukhtar, Z.Z.; Khosim, N.M.; Ramadhansyah, P.J.; Adiyanto, M.I.; Haziman, W.M. Prediction of Flexural Behavior of Woven Reinforced for Concrete Reinforcement. In *IOP Conference Series: Earth and Environmental Science*; IOP Publishing: Bristol, UK, 2021; Volume 682, p. 12052.
28. Kumar, A.; Arora, H.C.; Kumar, K.; Mohammed, M.A.; Majumdar, A.; Khamaksorn, A.; Thinnukool, O. Prediction of FRCC-Concrete Bond Strength with Machine Learning Approach. *Sustainability* **2022**, *14*, 845. [[CrossRef](#)]
29. Zhang, X.; Akber, M.Z.; Zheng, W. Prediction of seven-day compressive strength of field concrete. *Constr. Build. Mater.* **2021**, *305*, 124604. [[CrossRef](#)]
30. Niu, Y.; Cheng, H.; Wu, S.; Sun, J.; Wang, J. Rheological Properties of Cemented Paste Backfill and the Construction of a Prediction Model. *Case Stud. Constr. Mater.* **2022**, *16*, e01140. [[CrossRef](#)]
31. Congro, M.; de Alencar Monteiro, V.M.; Brandão, A.L.; dos Santos, B.F.; Roehl, D.; de Andrade Silva, F. Prediction of the residual flexural strength of fiber reinforced concrete using artificial neural networks. *Constr. Build. Mater.* **2021**, *303*, 124502. [[CrossRef](#)]
32. Sabapathy, Y.K.; Sabarish, S.; Nithish, C.N.A.; Ramasamy, S.M.; Krishna, G. Experimental study on strength properties of aluminium fibre reinforced concrete. *J. King Saud Univ.-Eng. Sci.* **2021**, *33*, 23–29. [[CrossRef](#)]
33. Kovačević, M.; Lozančić, S.; Nyarko, E.K.; Hadzima-Nyarko, M. Application of Artificial Intelligence Methods for Predicting the Compressive Strength of Self-compacting Concrete with Class F Fly Ash. *Materials* **2022**, *15*, 4191. [[CrossRef](#)]

-
34. Vincentdospital, T.; Toussaint, R.; Cochard, A. Thermal dissipation as both the strength and weakness of matter. A material failure prediction by monitoring creep. *Soft Matter* **2021**, *17*, 4143–4150.
 35. Lyngdoh, G.A.; Zaki, M.; Krishnan, N.A.; Das, S. Prediction of concrete strengths enabled by missing data imputation and interpretable machine learning. *Cem. Concr. Compos.* **2022**, *128*, 104414. [[CrossRef](#)]